Journal Title
XX(X):1–27

Reprints and permission:
sagepub.co.uk/journalsPermissions.nav
DOI: 10.1177/ToBeAssigned
www.sagepub.com/
SAGE

Observation of Edge Effect in Flexural Fatigue Test of Composites using Large Field of View Microscopy

Ulrich A. Mortensen[1], Tom L. Andersen[1], Lars P. Mikkelsen[1]

Abstract

Free-edge effects in fibre reinforced composites can produce premature damage at the composite edges due to mechanical, geometrical and hygro-thermal effects. Observation of damage on the free-edge of a composite plate is therefore different than what can be observed inside the material. The amount of individually broken fibres in a composite is counted by observing a test specimen with a polished edge and by cutting test specimens to observe damage inside the material. The amount of damage observed on a polished edge is found to greatly exceed that which is observed inside test specimens subjected to the same testing conditions. It is shown that the progression of important damage mechanisms can be observed on polished edges, but also that invalid damage mechanisms may be observed using free-edge microscopy.

Keywords

Fatigue, Micrscopy, Edge-effect, Basalt fibre

[1]Technical University of Denmark, Department of Wind Energy
Email: ulmo@dtu.dk

Introduction

Microscopy is a powerful tool for visual examination of different aspects of Fibre Reinforced Composites (FRC). Fibre architecture[1–3], manufacturing defects[4], and damage features such as matrix cracks[5], matrix-fibre debonding[6 7], delaminations,[8] and fibre breaks[9–11] can be inspected with microscopy with relatively low levels of magnifications. A commonly applied method used to inspect how damage evolves in FRC's is to observe the damage that develops on a polished edge or a polished surface of a composite laminate. These observations are commonly performed by interrupting mechanical tests during incremental static or cyclic loading, and then observing damage on the free polished edge or surface with a microscope before resuming the test. The mechanical test of a specimen is often interrupted several times, at pre-determined intervals, to observe edge or surface damage as it progresses during the static or fatigue loading. Many examples of these types of interrupted tests are available in the literature, and observations are either made on the in-plane surface of the composite material[6,11–13] or on machined and polished edges of the composite material[1,8,14–19]. While observations made on surfaces and edges may provide valuable insight into the damage and failure mechanism of composites, there is great chance that such results are influenced by mechanical edge-effects[20–22], which may cause premature damage initiation[20]. In addition to the existence of the mechanical effect that increases the severity of the load on a free edge, the polishing of a composite edge or surface may also produce effects that damage fibres on a micro-scale level. Fibres that lie in the same plane as the plane of observation are essentially polished such that their cross-sections become non-circular, which reduces their fracture resistance. Castro et al.[11] used a polished surface to quantify the number of broken fibres of a uni-directional (UD) glass-fibre composite. The study monitored fibre damage evolution during cyclic tension-tension fatigue experiments. Castro et al. observed that damage occurred more frequently near the polymeric stitching thread of the UD fabric, but also that breakage of fibres occurred at isolated positions away from the polymer thread, and away from clusters of other fibre breaks. Observations made in this study suggests that the occurrence of isolated fibre breaks may partially be an effect of observing them on a finely polished edge, on which a part of their original cross-section has been abrasively removed. Other effects, such as moisture, may also contribute to edge-effects since samples are often cleaned with alcohol-solutions prior to obtaining micrographs. Understanding the validity of observations made using microscopy is important for future research. The studies mentioned above should not be rendered invalid for using edges or surfaces for observation, yet there exists a need for knowledge of how observed damage on free-edge microscopy samples compares to microscopy observations of planes situated internally in the composite material of interest.

Another common challenge for microscopy examination of composite damage is to evaluate an area large enough to be representative for the material while retaining a level of magnification that reveals the micro-scale features that originally prompted the need for using a microscope. Most of the works mentioned above[1]-[13] limits the analysis to only include a single level of magnification and presents areas of interest without verification of how representative the given area is. Microscopy analysis such as those made by Edgren et. al[16] or Marsden[15] only allows observation of relatively[*] large intrabundle off-axis matrix cracks, disallowing analysis of damage types that are physically smaller. Findings made by Zangenberg et al[3] and Jespersen et al[23] suggest that stiffness degradation in UD non-crimp fabric composites are also affected by breakage of longitudinally oriented fibres, especially in areas near off-axis bundles with intrabundle matrix cracks. Zangenberg[3] and Jespersen[23] further suggests that fibre breaks in quasi-UD non-crimp fabrics are often related to transverse backing bundles. Observations of broken fibres with diameters of Ø10-Ø20 μm require levels of magnification that generally create fields of views that no longer covers areas large enough to include the structure of transverse fibre bundles, and can no longer be seen as representative for the damage state of the entire composite material.

[*]Relative size compared to single fibre diameter

Fatigue damage in composites is inherently a multi-scale phenomenon[10], and as such the methods that are used to observe how fatigue damage evolves must also have a modality that allows observations on all relevant scales of damage. Fatigue damage observations must furthermore come from planes of observation that are not influenced by unwanted effects, including edge-effects which are always present at free edges of composite laminates. This paper will present detailed microscopy observations over large fields of view in order to obtain data that is both representative and quantifiable. The Large Field of View (LFoV) microscopy method will provide images that cover areas from 36 mm^2 to roughly 100 mm^2, while allowing observation of micro-scale features such as broken fibres with diameters less than Ø20 μm. Two methods of microscopy observations – denoted as the edge observation method and the internal observation method, respectively - are applied to measure the amount of damage sustained by bending specimens during testing. The data shows that observations made on polished edges can provide qualitative insight into important damage mechanisms, but also that the quantitative data from polished edges exaggerate the amount of damage that exists internally in the composite material.

The data created for this work is available on-line in accordance with the FAIR Guiding Principles for scientific data management[24]. The data is available through two Zenodo † data sets; One for the internal observation micrographs[25] and one for the edge observation micrographs[26].

Methodology and Materials

Materials, Testing and Specimen Treatment

The composite material observed in this work was fabricated using a uni-directional non-crimp fabric, which is also sometimes denoted quasi-uni-directional fabric[27], made from basalt fibres. In the context of non-crimp fabrics, the designation of a *uni-directional* fabric embodies fabrics with a dominant direction (the 0° direction) of fibre

† An open-access repository under the OpenAIRE program and operated by CERN

bundles stitched together with a low amount of off-axis fibre bundles. The stitching thread is a thermoplastic polymeric thread[28]. In general, the fibre bundles in the 0°-direction have higher tex-valuesv[‡] than the off-axis bundles. Non-crimp fabrics are described by the area weight of the fibre bundles for each fibre direction, and for the specific material used in this study the area weight was 357 $\frac{g}{m^2}$ for the 0° fibres and 50 $\frac{g}{m^2}$ for the 90° off-axis bundles. The composite laminate was made with a symmetric stacking sequence $[0°]_{5s}$ where the side of the fabric with backing bundles was facing outwards from the center plane. This resulted in a plate with an average thickness of 3.61 mm. The in-plane longitudinal stiffness of the composite material was measured to 32.5 GPa and the fibre volume fraction was estimated to be 42 %.

The microscopy specimens described in the results sections were tested using the flexural fatigue testing method described by Mortensen[29] with rectangular specimens cut from the plate material described above. The test campaign applied a modified 4-point bending test fixture subjecting rectangular (180 mm by 20 mm by 3.6 mm) specimens to cyclic bending loads with a load ratio of $R = 0.1$ and a load frequency of 5 Hz. The applied 4-point bending fixture creates a loading area with a constant bending moment, and no shear force, over the length of the gauge area. The gauge area for the specimens is defined as the lengthwise span between the load rollers of the fixture, as shown in Figure 3a. The testing method produced consistent S-N curves - as shown in Figure 1 - and consistent damage in the gauge area of the specimens[29]. When subjecting a cross-section to bending loads the stress level in the material varies linearly through the thickness, from being zero at the center of the cross-section to reaching a maximum at the outer surface of the cross-section. For all micrographs, and sub-images of micrographs, shown in this paper the loading magnitude in the gauge area corresponds to exerting a maximum normal stress level of 325 MPa on the top and bottom surface. Figure 1 displays the S-N curve for the tests conducted by Mortensen[29] (marked by grey triangles ▲) showing that the stress level of 325 MPa is expected to cause failure of the microscopy samples after roughly 1 million load cycles. The blue ■

[‡]Linear Density measure of $\frac{g}{km}$

and red markers show the points at which the tests have been stopped or interrupted for microscopy observations. Each red triangle ( ) represents observations made on the edge of the same specimen after different amount sustained load cycles. The blue square points ( ) each represent one of 9 specimens tested to a fixed amount of cycles, before being cut to make observations internally in the specimens.

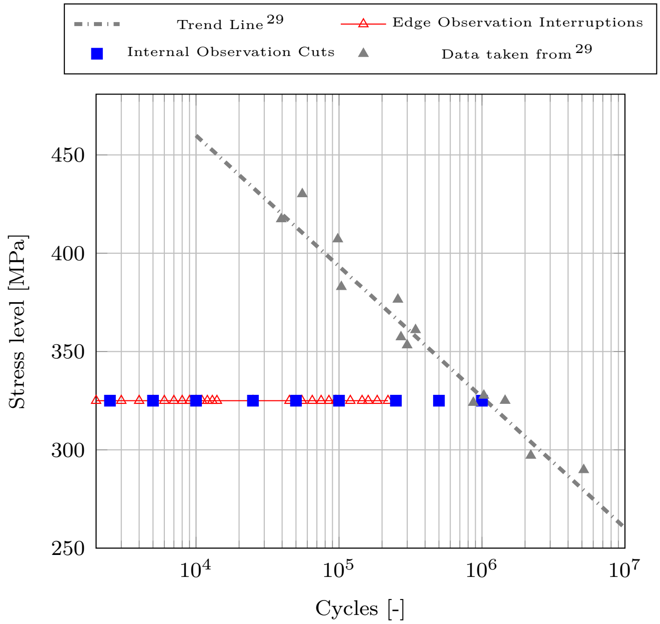

Figure 1. S-N curve with data from tests performed by Mortensen[29]. Points tests plotted for interruptions of the edge observation test specimen and for the stopped internal observation tests.

Microscopy Methodology

The Large Field of View (LFoV) microscopy images were acquired using a Leica DMI5000 microscope with an XY-stage capable of capturing micrographs in a grid format. The requirement for the level of observable details was determined by the microscale damage phenomena caused by the testing of the specimens. It was found that a 20 times magnification was needed in order to observe key damage features such as fibre breakage and debonding between fibre and matrix. Examples of fibre breaks and debonded fibres, caused by

fatigue loading, is showcased in Figure 2. The average diameter of the fibres are 17 μm, meaning that the 0.29 μm/pixel resolution of the images allows the width of the fibres to be resolved into roughly 60 pixels.
The images captured with the microscope have resolutions of 1536 by 2048 pixels, meaning that with a spatial pixel-resolution of 0.29 μm/pixel each image covers 0.45 mm by 0.59 mm. To cover 100 mm^2 with 20 percent overlap on all sides of the images requires 700-800 images. The xy-stage of the microscope allowed the images to be obtained automatically using a focus-mapping technique to account for the observation plane not being perfectly flat.

Stitching LFoV micrographs require a number of advanced image processing steps, including accurately predicting the translation from one sub-image to another. For this work, a MatLab script for image stitching was made instead of using commercially available software, as none of these gave satisfactory results in a sufficiently automated work-flow. The MatLab script used feature matching for image alignment combined with position data from the microscope, as well as implementation of several custom image processing steps. Notable details of the implementation are listed below.

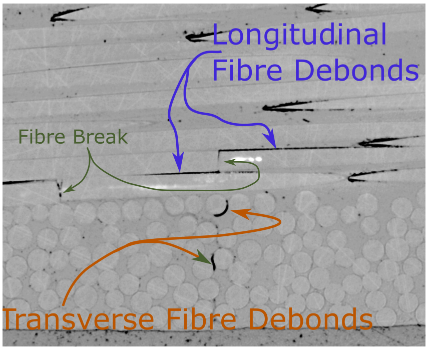

(a) Transverse and Longitudinal Fibre Debond

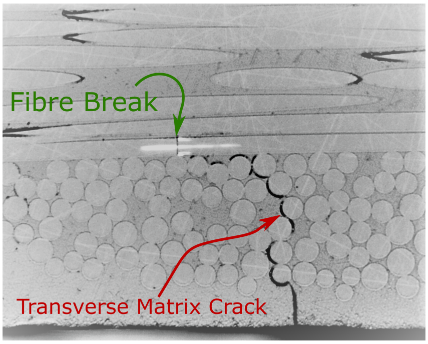

(b) Fibre breaks and transverse matrix cracks.

Figure 2. Visible details at the desired level of magnification observed using the internal observation method.

1. Correction of uneven background lighting using an image normalization process described by Chow et. al[30]. This technique was applied before feature registration.
2. Usage of both SURF[31] and Harris features[32] for image registration was found to work best for the specific microscopy images of this work. Compared to other types of feature detectors these provided the most amount of true pair feature matches, and with relatively few false positives.
3. Removal of false positives in feature matching by finding statistical outliers of the predicted image movement.

The stitched LFoV micrographs are available through Zenodo for both the edge observation LFoV micrographs[26] and the internal observation LFoV micrographs[25].

Edge damage observation and cut-out pieces for internal damage observations

The LFoV microscopy technique was used to observe fatigue damage in the composite materials by two methods that will be shown to provide quantifiably different results. The first method, which shall henceforth be denoted as the *Edge observation* method, was composed of polishing an edge of a test specimen, capturing a LFoV micrograph of the polished edge before any testing were performed, then subjecting the specimen to 1000 loading cycles, and then capturing a new LFoV micrograph of the same area. Repeated testing and acquisition of LFoV micrographs were performed until the specimen had lasted 1 Mill. loading cycles. The number of load cycles between capturing each LFoV micrograph was increased to 5,000 cycles interval after reaching 15,000 cycles, and further to intervals of 25,000 after reaching 45,000 cycles, and finally to 250,000 after reaching 225,000 cycles. The area observed using this method was roughly 10 mm long by 3.6 mm thickness (ie. roughly 36 mm^2 observation plane) as shown in Figure 3a. Between mechanical testing and microscopy observations, the edge observation specimen was cleaned with water. The cleaning procedure including wiping the specimen with ethanol and exposing the specimen to water for 1 minute, after which the specimen was blow-dried with

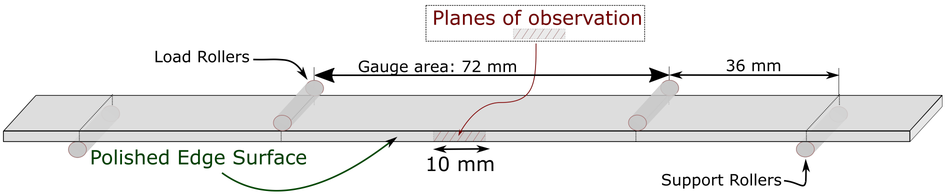

(a) The Edge observation method

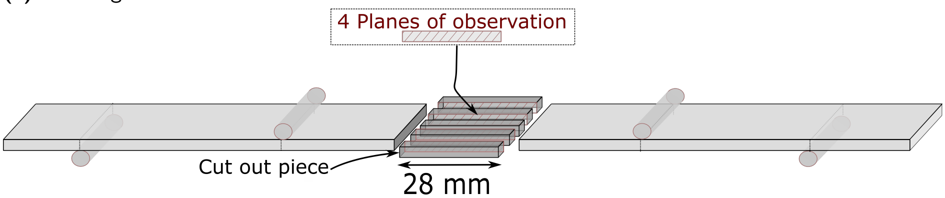

(b) The Internal observation method

Figure 3. Sketches of the plane of observation of the Edge observation method and the Internal observation method.

room temperature air. The cleaning process was always followed by the microscopy image acquisition process, leaving the specimen in laboratory conditions for 1-2 hours, but also frequently overnight (12-16 hours). The relatively short exposure to water compared to the time spend in controlled laboratory conditions makes it reasonable to assume that the moisture content on the polished edge had reverted to a near-equilibrium state before mechanical testing was resumed. In terms of general moisture content of all specimens, it should be noted that prior to cutting the test specimens the test material had been stored in laboratory conditions for at least 3 months.

The Edge observation method is advantageous because the same damage - i.e. crack, debonding or fibre break evolution - can be followed throughout the load history of a specimen. The specimen may, however, be affected by free-edge effects - both in terms of mechanical planar stress effects, environmental effects, and abrasive damage from surface polishing. The internal observation method are free of these uncertainties as the plane of observation are inside the material, but requires far more effort to get the same amount LFoV micrographs. X-ray microtomography encompasses the advantages of both methods, but the relatively low resolution and the time needed to create a 3D-volume image effectively limits the field of view to be lower than anything that can be considered representative with respect to non-crimp fabric composites. A study by Jespersen et al[28] have also shown that transverse matrix cracks are barely in x-ray tomography, and that fibre breaks may not be visible if the scanned specimens are not loaded in tension during the scan.

The plane of observation for all LFoV micrographs obtained in this study was oriented such that bottom of the image contains the area where the maximum tensile load prevailed in the specimen, while the top of the image contains the area where the maximum compressive load prevailed. Due to the nature of the bending load the middle of the image, i.e. between top and bottom, is where the stress transitions from compressive to tensile stress, and here the normal stress is zero.

Results

Large Field of View Images

Table 1. Overview of relative size and magnification[a] of the sequentially cropped sub-images shown in Figure 4.

Designation	True image Size		Pixel Resolution		Magnifaction	Percent of orignal Image
	Width	Length	Width	Height		
A	28.72 mm	4.06 mm	98764	13957	5.6	100.0
B	4.27 mm	2.88 mm	14688	9888	16.9	10.54
C	1.74 mm	1.13 mm	5999	3873	43.6	1.67
D	0.97 mm	0.20 mm	3328	685	164.3	0.17
E-1						
E-2	0.05 mm	0.05 mm	181	181	911.8	0.002
E-3						

Figure 4 shows an overview of the characteristics of a LFoV microscope image produced by the internal observation method, as well as the level of observable detail in a LFoV microscope image. The shown images are from a specimen tested with 10,000 cycles with a loading of 325 MPa at the specimen surfaces. Image A in Figure 4 depicts the full extent of a LFoV micrograph measuring a total of 28.7 mm by 4.1 mm[§]. Image B is a cropped area of image A, image C is a cropped area of image B and so forth. True and

[§]The Observed plane of the composite is 3.6 mm by 28 mm. The image size is larger in order to get the full piece into the LFoV area.

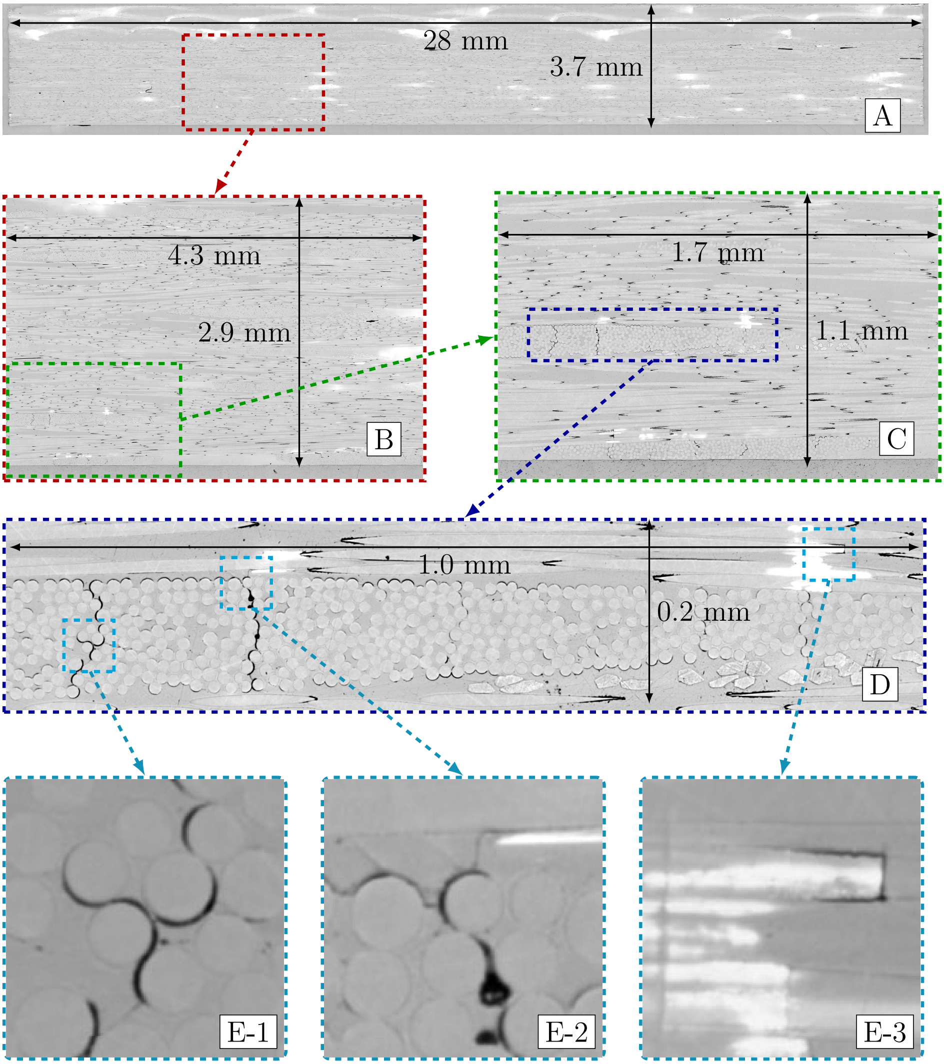

Figure 4. Sequential Magnification of LFoV micrograph based on the internal observation method

relative size, as well as relative magnification for each sub-image, is presented in Table 1. Image C in Figure 4 is the largest image that allows a level of detail where discernible features are visible. The bright white patches in image C are generally a sign of debonding of longitudinal fibres, and a careful inspection of image C will also reveal that the white patches are positioned in the immediate vicinity of areas with transverse bundles. As a more general statement, it should be noted that fibre breaks always occur near transverse fibre bundles that contain intrabundle matrix cracks, though this statement only holds for all LFoV micrographs captured with the internal method of observation. The transverse fibre bundles in image C do in fact contain transverse matrix cracks, this feature is emphasized in image D along with the white patches. In the left side of image D two distinct transverse matrix cracks are visible, but in the middle and to the right side of the image three more cracks are vaguely discernible in the image. Three features from image D are highlighted in images E-1 to E-3 which are all the same size, each covering only 0.002 percent of the original full LFoV micrograph. Image E-1 highlights a part of a transverse crack that is heavily influenced by the placement of the adjacent transverse fibres. Image E-2 displays both the interaction of a transverse intra-bundle matrix crack with the debonding of a longitudinal fibre. Image E-3 shows white patches, which is a sign of debonding immediately below the plane of observation, and several fibre breaks. Matrix cracks, fibre debonding, and fibre breakage as those shown in Images E-1 to E-3, are the damage features that are most commonly observed using the internal observation method.

Qualitative observations

The edge observation method, in which the same area of roughly 36 mm^2 is observed in between fatigue loading cycles, allows for following an area of damage progression in order to make a qualitative assessment of the damage mechanism(s) in the material. The edge observation images shown in Figure 5 shows the progression of the damage mechanism of transverse matrix cracking leading to fibre breaks over an area of of 0.81 mm by 0.77 mm (ie. 0.63 mm^2). The images are sub-images extracted near the tensionally loaded surface, which can be observed near the bottom of the LFoV micrographs. In Figure 5a the first fibre breaks occur near the transverse matrix cracks that are formed in the transverse backing bundle. The cracks are formed perpendicular to the tensile loading direction, and must as such be mode I cracks. The mode I crack in the bottom left of Figure 5a deflects as it reaches the longitudinal fibres, then then

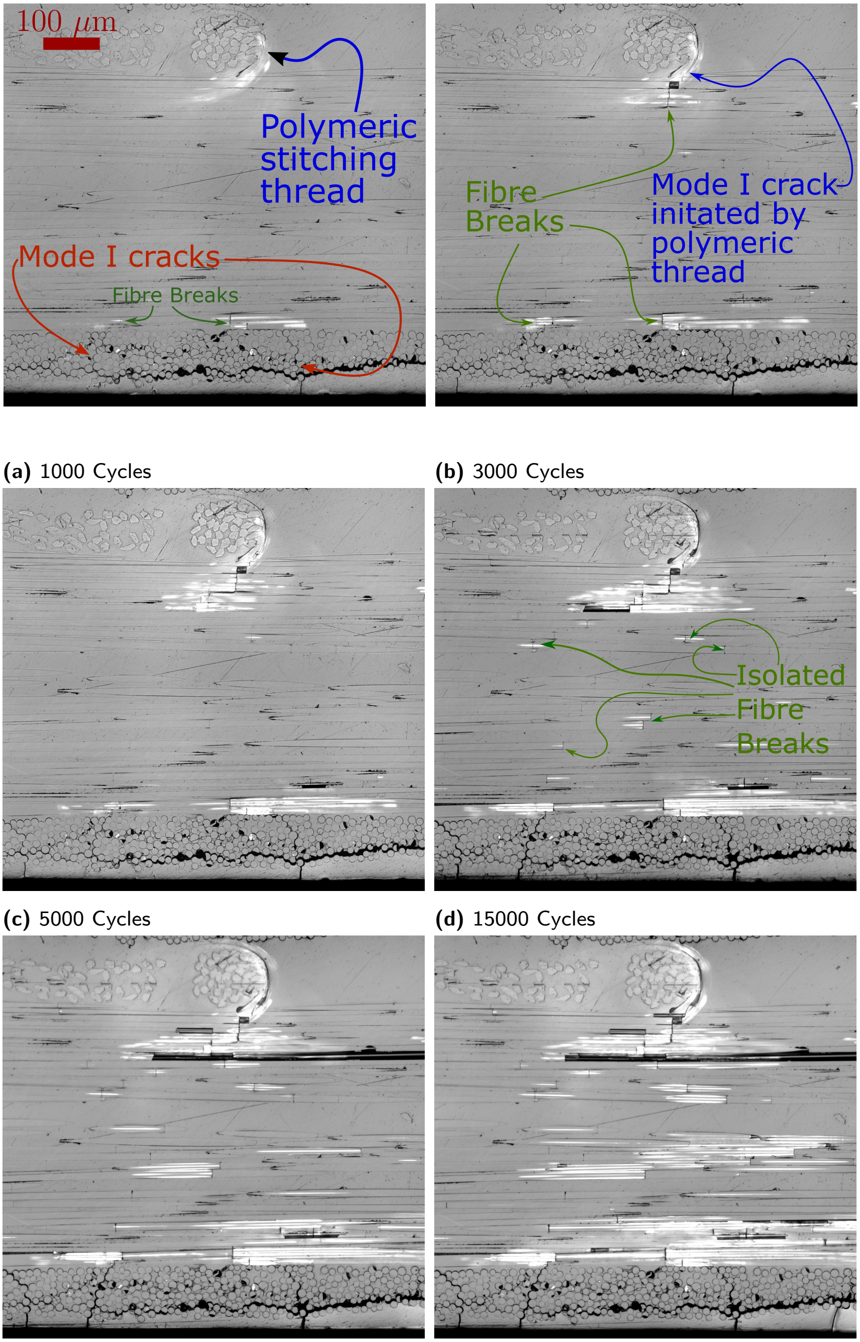

(a) 1000 Cycles **(b)** 3000 Cycles **(c)** 5000 Cycles **(d)** 15000 Cycles **(e)** 75000 Cycles **(f)** 225000 Cycles

Figure 5. Progression of damage for the edge observation method from 1,000 cycles to 225,000. The image is taken close to the tension surface, where the highest tensional loads exist.

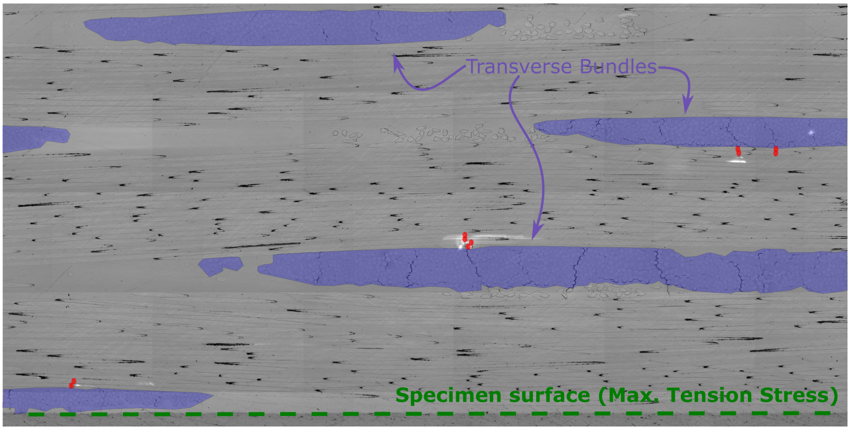

(a) The internal observation method (100,000 load cycles)

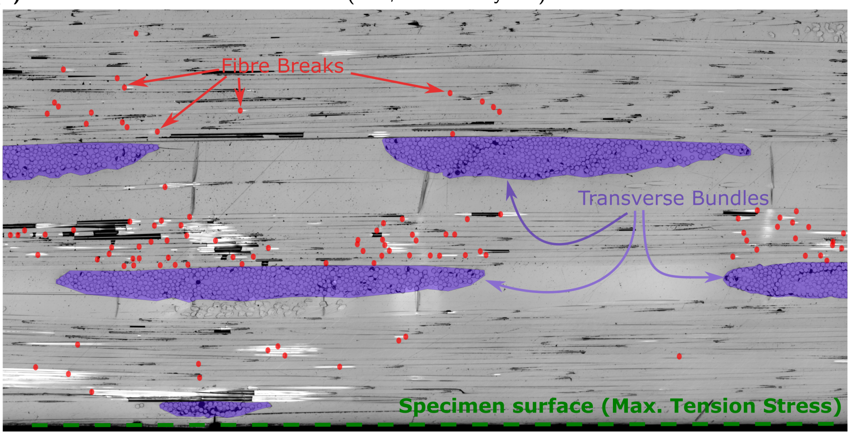

(b) The Edge observation method (95,000 load cycles)

Figure 6. Fibre breaks and transverse matrix bundles for the two methods of microscopy observation. Fibre break damage is marked with red spots. Both images covers the same physical area, and are taken at similar points in the fatigue life of the specimens.

propagates by debonding along the nearest longitudinal fibre which eventually leads to the breakage of said fibre, which followingly causes debonding along the neighbouring longitudinal fibre, which also breaks. These first fibre breaks, shown in Figure 5a, occur after only 1000 loading cycles and are consistent with the idea of fibre breaks occurring near transverse matrix cracks that exist in the transverse fibre bundles. The white patches near the fibre breaks are indications of debonding immediately underneath the observed surface. The damage shown in Figure 5b includes the progression of the damage shown in Figure 5a where the fibre break, in the bottom left near the transverse fibre bundle, has caused debonding and breakage of the adjacent longitudinal fibre. Figure 5b also includes a sequence of fibre breaks initiated from a mode I crack that originates from the polymeric thread used to sow together the longitudinal and transverse bundles of basalt fibres. While fibre break damage that originates from bundles of polymeric thread has only been observed in this one case, the example is included in order to generalize the dominant damage mechanism: Fibre breaks generally occur near mode I cracks. The reason that fibre breaks generally occur near the transverse backing bundles is that mode I cracks most frequently occur inside the transverse backing bundles. The fibre break sequence originating from the polymeric thread is also a clear example of how the damage progresses once longitudinal fibres break. Inspecting the damage progression from 3000 cycles (Figure 5b) to 5000 cycles (Figure 5c) and then finally to 15000 cycles (Figure 5d) shows how debonding near a broken fibre is transferred to an adjacent fibre, which then breaks in a new place in the longitudinal direction after a certain length of debonding. This mechanism, where fibre breaks are initiated from mode I cracks and damage progresses as series of subsequent fibre debonding and fibre breakage is consistent with the damage mechanism proposed by Zangenberg[3] and observed through micro tomography by Jespersen et al.[27,28]. After 15000 cycles (Figure 5d) fibre breaks are frequently appearing in areas that are not linked to transverse bundles. This trend is only present in the images captured for the edge observations. In the observations made using the internal observation method the fibre break damage does not occur in positions isolated from damage regions that originated from transverse backing bundles.

Figure 6 shows two sub-images, one from the internal observation method and one from the edge observation method, that are of the exact same size, and extracted from similar locations with similar structures - ie. a transverse backing bundle near the surface and fibre breaks in the longitudinal fibre bundles. There are two distinct differences between Figure 6a and Figure 6b; the first is that there is a significantly greater number of fibre breaks (marked by red dots) in Figure 6b than in Figure 6a. The other notable difference is that in Figure 6b the fibre breaks are scattered all over the area where there are longitudinal fibres, while in Figure 6a the fibre breaks are all positioned close to each other in a cluster that lies close to a transverse fibre bundle. The crack openings in the transverse bundles in Figure 6b is slightly more severe than the cracks of the transverse bundle in Figure 6a, which is a possible explanation for the increased number of fibre breaks. In general, it was observed that transverse cracks in the edge observation specimens were more open, especially in bundles close to the tension surface, than the transverse cracks in the internal observation specimens. Furthermore, the more severe damage state in the transverse bundles observed with the edge observation method does not explain the isolated positions of the fibre breaks, and is thus not a comprehensive explanation for the significantly higher number of fibre breaks observed using the edge observation method. The position of the fibre breaks observed for the internal observation method is generally in compliance with observations made by Jespersen et al.[27] and the general damage mechanism observed and postulated by Zangenberg et al.[3].

As an intrinsic property of the bending loads imposed on the test specimens only half of the observed areas of the LFoV micrographs have been subjected to linearly varying tensile load, while the other half have been subjected linearly varying compressive loads. As a property of this loading situation, the described damage mechanism can not be present in the half of the specimen that have been subject to compressive loading, as this damage mechanism relies on mode I cracks which do not occur under compressive loading. This assertion fits with only a single observation of a broken fibre in a compressively loaded are through all the LFoV micrographs captured with the internal observation method. For the edge observation method this assertion does not hold as a small, but not insignificant, number of fibre breaks were observed in areas of the micrograph where compressive stresses must have prevailed.

Quantitative observations

The qualitative observations indicate that a significantly larger number of fibre breaks are present at the specimen edges than inside the material. The stiffness degradation of the material is related to damage sustained in the material, which includes transverse matrix cracks and fibre breaks. In most composites, with significant amounts of off-axis fibres, the main cause of stiffness degradation is transverse cracks. This is especially true for cross-ply laminates, but does not hold for composites based on quasi-UD non-crimp fabrics, such as the material tested in this work. The stiffness degradation caused by transverse cracks are limited for quasi-UD composites. Zangenberg[3] showed that, for composite materials made from quasi-UD non-crimp fabrics, the stiffness loss from cracks in transverse backing bundles could account for only a very small part of the stiffness degradation. Zangenberg[3] further documented that the stiffness loss in fatigue loading of quasi-UD non-crimp fabric composites is directly related to fibre breaks in the load-carrying axial fibre bundles. The current material can also be classified as a quasi-UD non-crimp fabric composite, however, it is made with a fabric with a relatively higher amount of backing bundles than the one investigated by Zangenberg[3]. Replicating the stiffness model used by Zangenberg[3] for the fabric used in this study indicate that the loss in axial stiffness can not amount to more than 1.55 % of the original stiffness, under the assumption that the load carrying capability of the transverse bundles is completely lost. The degradation of the material stiffness after 250,000 load cycles amounts to approximately 3-4 %, which means that it is reasonable to assume that both the transverse cracks and the fibre breaks contribute to the stiffness loss. Fibre breaks are furthermore a distinct and countable feature in the LFoV micrographs, whereas the transverse cracks are more difficult to quantify. These properties make fibre breaks a reasonable feature for quantification of damage magnitude in the LFoV captured with both the edge observation method and the internal observation method. Because the transverse cracks have more variation, in terms of discrete counting, than the fibre breaks, the quantitative observations will be based on counted fibre breaks rather than transverse cracks. It must, however, be noted that the fibre breaks can not be regarded as the sole cause for stiffness degradation in the material, as there is also a significant contribution from the transverse cracks.

Figure 7 shows the apparent stiffness loss of the edge polished specimen and the specimens tested and then cut out to use for the internal observation method. The stiffness loss is here defined as the loss in normalized stiffness modulus. The normalized stiffness modulus is the instantaneous stiffness E modulus over the stiffness modulus recorded during the first 100 loading cycles E_0. The stiffness loss for the two methods are similar for the first 250,000 cycles. The stiffness loss for the edge observation specimen is 3.2 % after 225,000 cycles. For the internal observation specimen stopped after 250,000 cycles the recorded stiffness loss was 3.9 %. After 250,000 cycles there is a significant stiffness drop for both types of specimens, which could be a result of a new damage type appearing at this stage of the fatigue life. Consequently the quantitative analysis of the number of fibre breaks will be performed for data collected in this load cycle range.

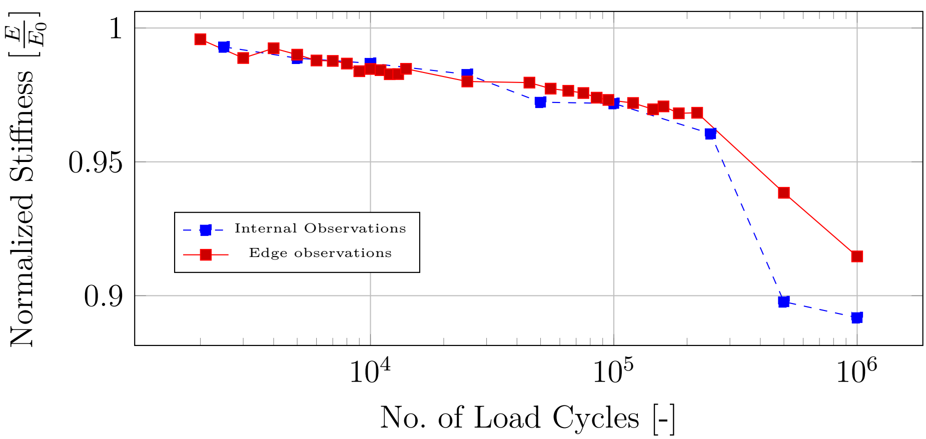

Figure 7. The loss in normalized stiffness $\frac{E}{E_0}$ plotted as a function of the number of sustained loading cycles. Internal observations are measures from independent test specimens. Edge observation are measurement from the same specimen at each point of microscopy analysis.

The higher number of fibre breaks in the edge observation specimens compared to the internal observation specimens can be visualized by plotting the quantified fibre breaks against the number of applied loading cycles. Figure 8 shows a significant difference in the number of observed fibre breaks found using the edge method compared to the internal method. The significantly greater number of fibre breaks observed on the edge of the specimen is consistent with the qualitative observations, though the relative number of fibre breaks observed on the edge compared to the number of fibre breaks observed internally in the material is more extreme than anticipated.

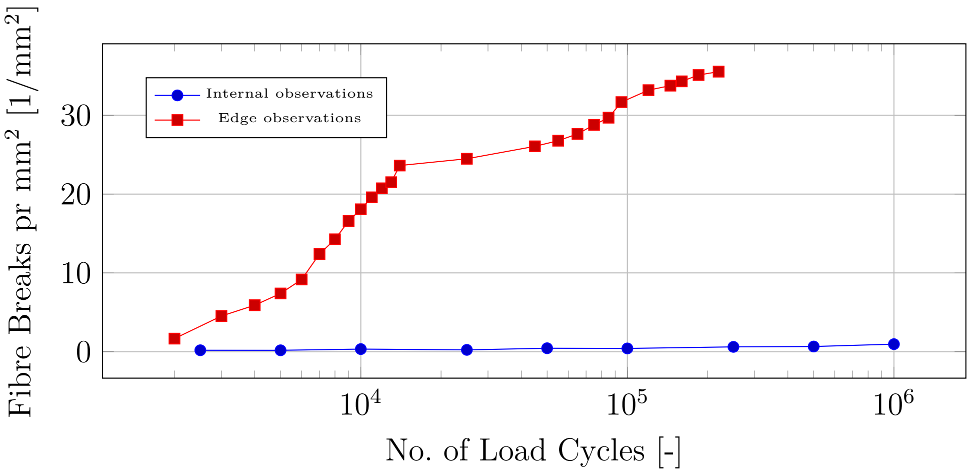

Figure 8. The number of manually counted fibre breaks plotted as a function of the number of sustained loading cycles.

In quasi-UD non-crimp fabric, where fibre breaks can not be disregarded in relation to the material stiffness degradation[28], an analysis based on edge observations would greatly underestimate the influence of fibre breaks on the loss of material stiffness. To estimate how greatly the effect of fibre breaks would be underestimated it is useful to see the relation between fibre breaks and stiffness loss, even though the stiffness degradation is also affected by transverse cracking in the transverse fibre bundle. This information is depicted in Figure 9, where the upper graph show how many fibre breaks occur for a normalized flexural stiffness loss. The upper graph contains data for both the edge fibre breaks and the internal fibre breaks, while the lower graph details the data for the internal fibre breaks. The filled circles show the mean number of fibre breaks pr. area over each of the 4 planes of observation available from each of the 9 specimens, while the empty circles show the mean value for each individual plane of observation. Though both methods show a linear relation between the loss of flexural stiffness and the quantity of fibre breaks, the trend for the edge method is > 200 times higher than for the internal observation method. The number of fibre breaks observed on the edge of the specimen obviously overstate the actual number of fibre breaks in the specimen. The internal observation method provides a far more accurate representation of the number of fibre breaks in the material.

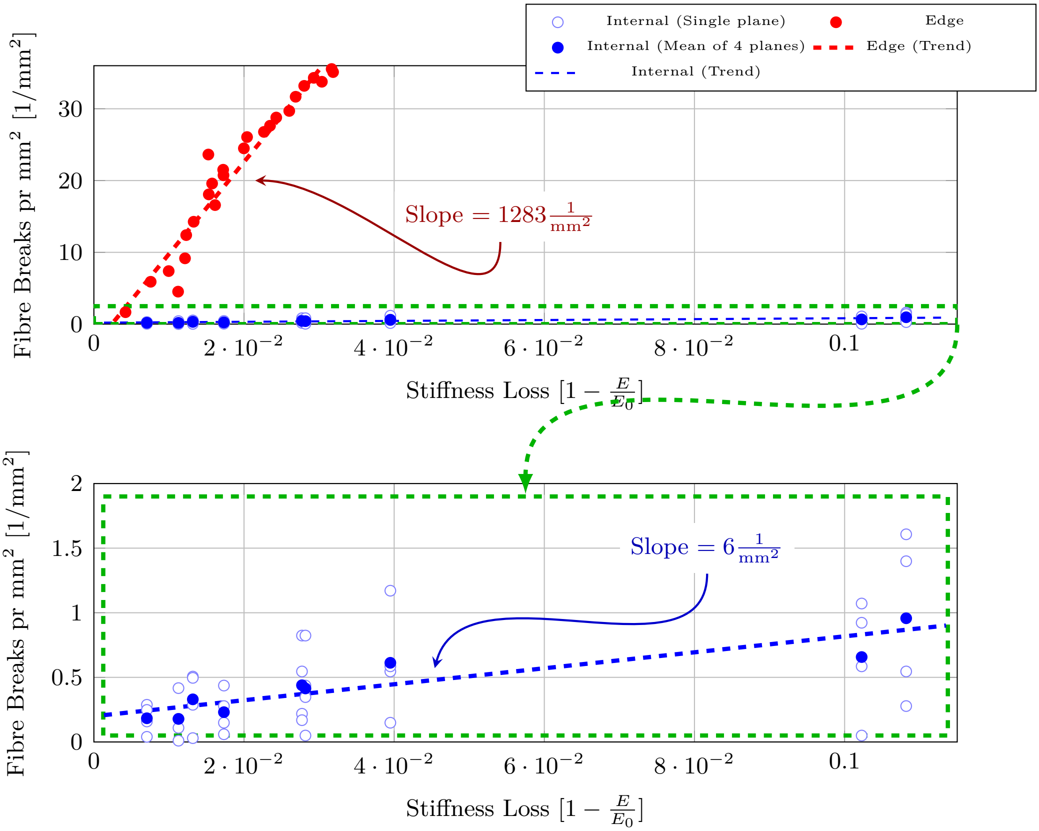

Figure 9. The number of fibre breaks related to the loss in normalized stiffness $\frac{E}{E_0}$. Fibre breaks are only partly responsible for the loss in material stiffness.

Discussion & Conclusion

Discussion

The presented results provides information and knowledge regarding the methodologies - the edge observation and the internal observation microscopy methods - applied in this study, but also qualitative and quantitative information about the damage mechanism that causes stiffness degradation in non-crimp fabric composites due to bending loads. The quantitative data have shown that the amount of damage observed on a polished edge of a test specimen is likely to be excessive compared to what exists inside the material. It is reasonable to believe that the damage mechanism presented in Figure 5 is generally valid because the described damage progression is consistent with observations made inside the material - ie. the observed fibre breaks occur near transverse bundles with mode I cracks. In contrast, the isolated fibre breaks observed on the material edge are rarely observed inside the material and can as such be assumed to be a product of what is commonly denoted in the literature as edge effects or free-edge effects. In the context of the current experiment, the term *edge effects* should be understood in the broadest sense of the expression such that it includes mechanical free-edge effects, see e.g.[21 22], as well as environmental factors such as hygro-thermal effects.

In terms of hygro-thermal loading a main source of concern is the washing of the polished side of the observed specimen: In order to avoid smudge and debris, which inevitably intrudes the polished surface during testing of the specimen, the specimen was cleaned using water and ethanol before LFoV microscopy images were captured. The cleaning procedure is necessary to avoid debris on the microscopy sample, though it may be part of the observed edge effect. It is, however, important to note that the specimen was cleaned multiple times before subjecting it to any mechanical load, and no fibre break damage or debonding damage was observed in the LFoV microscopy obtained after the cleaning and before testing. and as such the effect must be a second-order effect. However, the relatively short exposure to water followed by a significantly larger amount of time spent in laboratory condition is expected to have significantly reduced any effect that could otherwise promote mechanical damage at the edge of the specimen. Furthermore, while moisture uptake in composites generally produces internal stresses[33], most composite materials, including the one investigated in this study, are affected by thermally induced residual stresses from the curing procedure which are relieved to some extent by moisture uptake[34]. Thus a small amount of moisture uptake at the polished edge could relieve some residual stresses, and thereby lower the effect of moisture. It should also be noted that the specimens made for the internal observation method have been cleaned multiple times with the same procedure and no additional damage have been observed in those specimens as a direct implication of the cleaning. With respect to the edge polishing, it is also worth considering that the finely polished surface - 1 μm grains were used at the finest level - are made up by fibres that have in essence been cut in half by the polishing, which may significantly reduce their resistance to breakage. While this effect of polishing away significant portions of fibres located on the surface is not relevant for microscopy observations mostly focussed on matrix cracks (e.g.[16 35 14 19]), there are several studies in the literature where it remains a valid concern (e.g.[11 6 13]).

The results show that quantifying the damage observed on a polished edge would greatly overestimate how much damage is necessary for a given stiffness degradation of the material and hence overestimate the damage tolerance of the material. The governing damage mechanism, where mode I cracks in transverse fibre bundles lead to fibre breaks, are, however, present in both the images captured on the polished edge of the material, but also the observations made inside the material. As such, there is good reason to believe that the observations made in relation to this damage mechanism are qualitatively sound. It is, however, only because the edge observations have been compared with the internal observations that it is reasonable to conclude that the damage mechanism is generally valid. Though observations made on polished edges or surface are common in the literature[1,6,8,11–17], validation by microscopy observation inside the same material is a rare occurrence.

Conclusion

In the current study, a large quantity of large field of view micrographs, spanning over representative areas, has been examined qualitatively and quantitatively. Two different methodologies have been applied. Significantly different quantitative results have been presented for observations made inside the material compared to edge observations. The difference between the results observed on a polished edge of a specimen compared to observations made inside the material are caused by a free-edge effect.

The most significant qualitative observations made on the edge surface are consistent with those made inside the material. The specific observation is a damage mechanism where intrabundle matrix cracks in transverse backing bundles interact with load carrying longitudinal fibres. The longitudinal fibres near matrix cracks suffer first from some degree of debonding, and subsequently from brittle failure of the fibre itself. Once the fibre closest to the transverse fibre bundle has failed it causes debonding of adjacent fibres, which then also fractures and then continues the pattern. This failure mechanism is consistent with observations made by Zangenberg et al[3] and Jespersen et. al[23 28], and have been validated in this very study by LFoV micrograph observations made inside the material. Further validation of the damage mechanism using the relative position of the quantified fibre breaks with respect to the transverse bundles will be investigated in a future work[36].

Generally it can be stated that; Damage observed on a polished surface of a specimen subjected to cyclic mechanical load are influenced by a free-edge effect, such that the amount of observed damage far exceeds the damage inside the material. Furthermore, it can be stated that; Edge observation studies may be applied to qualitatively asses the development of a damage mechanism over the fatigue life of a specimen, though caution must be taken as the extent of the damage is greater than that which may be found inside the observed sample.

References

1. Kim H and Ebert L. Flexural fatigue behaviour of unidirectional fibreglass composites. *Fibre Science and Technology* 1981; 14: 3 – 20.
2. Beauson J, Markussen C and Madsen B. Analysis of composition and microstructural uniformity of hybrid glass/carbon fibre composites. *Proceedings of the Risø International Symposium on Materials Science* 2013; 34: 177–191.
3. Zangenberg J, Brøndsted P and John W Gillespie J. Fatigue damage propagation in unidirectional glass fibre reinforced composites made of a non-crimp fabric. *Journal of Composite Materials* 2014; 48(22): 2711–2727. DOI:10.1177/0021998313502062. URL `https://doi.org/10.1177/0021998313502062`. `https://doi.org/10.1177/0021998313502062`.
4. Paciornik S and D'Almeida J. Measurement of void content and distribution in composite materials through digital microscopy. *Journal of Composite Materials* 2009; 43(2): 101–112. DOI:10.1177/0021998308098234. URL `https://doi.org/10.1177/0021998308098234`.
5. Lafarie-Frenot M, Hénaff-Gardin C and Gamby D. Matrix cracking induced by cyclic ply stresses in composite laminates. *Composites Science and Technology* 2001; 61(15): 2327 – 2336. DOI:https://doi.org/10.1016/S0266-3538(01)00125-7. URL `http://www.sciencedirect.com/science/article/pii/S0266353801001257`.
6. Gamstedt E, Berglund LA and Peijs T. Fatigue mechanisms in unidirectional glass-fibre-reinforced polypropylene. *Composites Science and Technology* 1999; 59(5): 759 – 768. DOI:https://doi.org/10.1016/S0266-3538(98)00119-5. URL `http://www.sciencedirect.com/science/article/pii/S0266353898001195`.
7. Jollivet T and Greenhalgh E. Fractography, a powerful tool for identifying and understanding fatigue in composite materials. *Procedia Engineering* 2015; 133: 171 – 178. DOI:https://doi.org/10.1016/j.proeng.2015.12.646. URL `http://www.sciencedirect.com/science/article/pii/S1877705815045658`. Fatigue Design 2015, International Conference Proceedings, 6th Edition.
8. Reifsnider K. Fatigue behavior of composite materials. *International Journal of Fracture* 1980; 16(6): 563–583. DOI:10.1007/BF02265218. URL `https://doi.org/10.1007/BF02265218`.
9. Shih G and Ebert L. The effect of the fiber/matrix interface on the flexural fatigue performance of unidirectional fiberglass composites. *Composites Science and Technology* 1987; 28(2): 137 – 161. DOI:http://dx.doi.org/10.1016/0266-3538(87)90095-9. URL `http://www.sciencedirect.com/science/article/pii/0266353887900959`.
10. Quaresimin M. A damage-based approach for the fatigue design of composite structures. *IOP Conference Series: Materials Science and Engineering* 2016; 139(1): 012006. URL `http://stacks.iop.org/1757-899X/139/i=1/a=012006`.
11. Castro O, Carraro PA, Maragoni L et al. Fatigue damage evolution in unidirectional glass/epoxy composites under a cyclic load. *Polymer Testing* 2019; 74: 216 – 224. DOI:https://doi.org/10.1016/j.polymertesting.2018.12.027. URL `http://www.sciencedirect.com/science/article/pii/S0142941818319202`.

12. Quaresimin M, Carraro P and Maragoni L. Early stage damage in off-axis plies under fatigue loading. *Composites Science and Technology* 2016; 128: 147 – 154. DOI:https://doi.org/10.1016/j.compscitech.2016.03.015. URL http://www.sciencedirect.com/science/article/pii/S0266353816301026.
13. Gamstedt EK and Talreja R. Fatigue damage mechanisms in unidirectional carbon-fibre-reinforced plastics. *Journal of Materials Science* 1999; 34(11): 2535–2546. DOI: 10.1023/A:1004684228765. URL https://doi.org/10.1023/A:1004684228765.
14. Paepegem WV and Degrieck J. Coupled residual stiffness and strength model for fatigue of fibre-reinforced composite materials. *Composites Science and Technology* 2002; 62(5): 687 – 696. DOI:https://doi.org/10.1016/S0266-3538(01)00226-3. URL http://www.sciencedirect.com/science/article/pii/S0266353801002263.
15. Marsden C, Li C, Biernacki M et al. 4-point bending fatigue testing of thin carbon-epoxy laminates. *Proceedings of the 19th International Conference on COmposite Materials* 2013; .
16. Edgren F, Mattsson D, Asp LE et al. Formation of damage and its effects on non-crimp fabric reinforced composites loaded in tension. *Composites Science and Technology* 2004; 64(5): 675 – 692. DOI:https://doi.org/10.1016/S0266-3538(03)00292-6. URL http://www.sciencedirect.com/science/article/pii/S0266353803002926.
17. Mattsson D, Joffe R and Varna J. Damage in ncf composites under tension: Effect of layer stacking sequence. *Engineering Fracture Mechanics* 2008; 75(9): 2666 – 2682. DOI:http://dx.doi.org/10.1016/j.engfracmech.2007.03.014. URL http://www.sciencedirect.com/science/article/pii/S0013794407001129. Fracture of Composite Materials.
18. Takeda N, Kobayashi S, Ogihara S et al. Experimental characterization of microscopic damage progress in quasi-isotropic cfrp laminates: effect of interlaminar-toughened layers. *Advanced Composite Materials* 1998; 7(2): 183–199. DOI: 10.1163/156855198X00138. URL https://doi.org/10.1163/156855198X00138.
19. Pakdel H and Mohammadi B. Experimental observation and energy based analytical investigation of matrix cracking distribution pattern in angle-ply laminates. *Theoretical and Applied Fracture Mechanics* 2017; 92: 146 – 154. DOI:https://doi.org/10.1016/j.tafmec.2017.06.007. URL http://www.sciencedirect.com/science/article/pii/S0167844216304049.
20. Zhang C and Binienda WK. A meso-scale finite element model for simulating free-edge effect in carbon/epoxy textile composite. *Mechanics of Materials* 2014; 76: 1 – 19. DOI:https://doi.org/10.1016/j.mechmat.2014.05.002. URL http://www.sciencedirect.com/science/article/pii/S0167663614000969.
21. Lecomte-Grosbras P, Paluch B and Brieu M. Characterization of free edge effects: influence of mechanical properties, microstructure and structure effects. *Journal of Composite Materials* 2013; 47(22): 2823–2834. DOI:10.1177/0021998312458817. URL https://doi.org/10.1177/0021998312458817.
22. Hosoi A, Yagi S, Nagata K et al. Interaction between transverse cracks and edge delamination considering free-edge effects in composite laminates. *ICCM International Conferences on Composite Materials* 2007; URL

https://www.scopus.com/inward/record.uri?eid=2-s2.0-79960033851&partnerID=40&md5=70c53b25d0b0954b036305846d6aaa33.

23. Jespersen KM, Zangenberg J, Lowe T et al. Fatigue damage assessment of uni-directional non-crimp fabric reinforced polyester composite using x-ray computed tomography. *Composites Science and Technology* 2016; 136: 94 – 103. DOI:https://doi.org/10.1016/j.compscitech.2016.10.006. URL http://www.sciencedirect.com/science/article/pii/S0266353816314130.
24. Wilkinson M and et al. The fair guiding principles for scientific data management and stewardship. *Nature Scientific Data* 2016; (160018). URL http://www.nature.com/articles/sdata201618.
25. Mortensen UA, Andersen TL and Mikkelsen LP. Internal large field of view observations with optical microscope of fatigue damage in composite materials during bending loading [data set]. zenodo., 2019. DOI:http://doi.org/10.5281/zenodo.2643445. URL http://doi.org/10.5281/zenodo.2643445. Doi: 10.5281/zenodo.2643445.
26. Mortensen UA, Andersen TL and Mikkelsen LP. Edge based large field of view observations with optical microscope of fatigue damage in composite materials during bending loading [data set]. zenodo., 20019. DOI:http://doi.org/10.5281/zenodo.2643947. URL http://doi.org/10.5281/zenodo.2643947. Doi: 10.5281/zenodo.2643947.
27. Jespersen KM and Mikkelsen LP. Three dimensional fatigue damage evolution in non-crimp glass fibre fabric based composites used for wind turbine blades. *Composites Science and Technology* 2017; 153: 261 – 272. DOI:https://doi.org/10.1016/j.compscitech.2017.10.004. URL http://www.sciencedirect.com/science/article/pii/S0266353817301811.
28. Jespersen KM, Glud JA, Zangenberg J et al. Uncovering the fatigue damage initiation and progression in uni-directional non-crimp fabric reinforced polyester composite. *Composites Part A: Applied Science and Manufacturing* 2018; : –DOI:https://doi.org/10.1016/j.compositesa.2018.03.002. URL https://www.sciencedirect.com/science/article/pii/S1359835X18300964.
29. Mortensen UA. Fatigue damage in non-crimp fabric composites subjected to cyclic bending load. *Proceedings of the 2nd International Symposium on Multiscale Experimental Mechanics* 2017; URL http://www.casmat.dtu.dk/activities/symposiums/ismem-2017/papers.
30. CHOW SK, HAKOZAKI H, PRICE DL et al. Automated microscopy system for mosaic acquisition and processing. *Journal of Microscopy* 2006; 222(2): 76–84. DOI:10.1111/j.1365-2818.2006.01577.x.
31. Bay H, Tuytelaars T and Van Gool L. Surf: Speeded up robust features. In Leonardis A, Bischof H and Pinz A (eds.) *Computer Vision – ECCV 2006*. Berlin, Heidelberg: Springer Berlin Heidelberg. ISBN 978-3-540-33833-8, pp. 404–417.
32. Harris CG, Stephens M et al. A combined corner and edge detector. In *Alvey vision conference*. Number 50 in 15, Citeseer, pp. 10–5244.
33. Joliff Y, Rekik W, Belec L et al. Study of the moisture/stress effects on glass fibre/epoxy composite and the impact of the interphase area. *Composite Structures*

2014; 108: 876 – 885. DOI:https://doi.org/10.1016/j.compstruct.2013.10.001. URL `http://www.sciencedirect.com/science/article/pii/S026382231300514X`.

34. Vaddadi P, Nakamura T and Singh RP. Transient hygrothermal stresses in fiber reinforced composites: a heterogeneous characterization approach. *Composites Part A: Applied Science and Manufacturing* 2003; 34(8): 719 – 730. DOI:https://doi.org/10.1016/S1359-835X(03)00135-0. URL `http://www.sciencedirect.com/science/article/pii/S1359835X03001350`.
35. Mattsson D, Joffe R and Varna J. Methodology for characterization of internal structure parameters governing performance in ncf composites. *Composites Part B: Engineering* 2007; 38(1): 44 – 57. DOI:https://doi.org/10.1016/j.compositesb.2006.04.004. URL `http://www.sciencedirect.com/science/article/pii/S135983680600076X`.
36. Mortensen UA, Andersen TL and Mikkelsen LP. Observations of fatigue damage in uni-directional non-crimp fabric composites subjected to cyclic bending loads. *Submitted to Composites Part A* 2019; N/A.